



EUMETSAT/ECMWF Fellowship Programme Research Report

66

Quality Assessment of IASI 3D Winds

Francis Warrick
October 2025

Report Research Report
ogramme EUMETSAT/ECM
arch Report Research Report
Programme EUMETSAT/E
esearch Report Research F
ship Programme EUMETSA
ERESearch Report Research
owship Programme EUME
port Research Report Research
Fellowship Programme EU
Report Research Report F
WF Fellowship Programme

search Report Research Report Research Report Research Report Fellowship Programme EUMETSAT/ECMWF Fellowship Program Research Report Research

Series: EUMETSAT/ECMWF Fellowship Programme Research Reports

A full list of ECMWF Publications can be found on our web site under:

http://www.ecmwf.int/en/publications/

Contact: library@ecmwf.int

© Copyright 2025

European Centre for Medium Range Weather Forecasts, Shinfield Park, Reading, RG2 9AX, UK

Literary and scientific copyrights belong to ECMWF and are reserved in all countries. The content of this document is available for use under a Creative Commons Attribution 4.0 International Public License. See the terms at https://creativecommons.org/licenses/by/4.0/.

The information within this publication is given in good faith and considered to be true, but ECMWF accepts no liability for error or omission or for loss or damage arising from its use.



Abstract

A 4-month test dataset of novel wind vectors derived from the IASI level 2 profiles was made available by EUMETSAT. These provide wind profile information at mid and high latitudes, in the areas of overlap between successive Metop-B and Metop-C IASI swaths. The IASI winds are derived using the optical flow technique simultaneously on ozone, humidity and temperature retrievals on 25 fixed pressure layers. The test data was passed through IFS to generate background departures (i.e., differences between the observations and a short-range forecast), without assimilating the IASI winds. The departure statistics indicated a widespread and often large slow bias compared to the ECMWF background. The smallest background departures were seen in the low stratosphere pressure layers, the largest around the tropopause. For the troposphere, root mean squared errors against the ECMWF background were overall significantly larger than values for traditional AMVs currently assimilated in the ECMWF system, suggesting larger errors in the IASI winds. It is noted that information on the data quality characteristics should be added in the disseminated dataset, for instance in the form of a quality indicator for each derived wind, as well as information on whether the AMV was derived from cloudy or clear-sky scenes, in order to enable better quality control of the data, independent of a model background.

1 Introduction to 3D Winds

Atmospheric Motion Vectors (AMVs) are a key part of the global observing system, providing much needed wind data coverage in data-sparse regions and delivering a significant improvement to forecast skill when assimilated into NWP models. They have many limitations however, including difficulties with assigning a height to the tracked motion, providing a wind measurement only at a single layer rather than a profile, requiring strong brightness contrasts for the cross-correlation tracking to work, and not measuring the vertical wind.

The motivation of developing a 3D winds product is both to address traditional AMVs' limitations and to ensure that maximum possible value is extracted from sensors such as Infrared Atmospheric Sounding Interferometer (IASI) on the polar-orbiting Metop satellites, and the upcoming InfraRed Sounder (IRS) on the geostationary MTG-S1 satellite. EUMETSAT's IASI 3D winds product aims to do this by extracting a gapless 3D wind field consisting of a stack of standard pressure layers derived from IASI temperature, ozone and humidity retrievals.

Previous 3D winds research has included feature tracking on humidity retrievals from simulated IRS data [9]. This work demonstrated the feasibility of the deriving winds that are reasonably similar to the Met Office model background using IRS data, and found that smoothing the retrieved IRS fields and carefully tuning the derivation parameters was important for deriving good quality AMVs. A similar approach using AIRS ¹ humidity and ozone retrievals [7] found good agreement with clear-sky MODIS ² water vapour channel AMVs, a slightly positive but not statistically significant impact from assimilating the AIRS winds. This approach was then extended to CrIS ³, and the resulting AMVs had a good agreement with ERA5 wind fields [8]. Note that the AIRS and CrIS winds made use of a model first-guess to aid the tracking and both they and the simulated IRS winds tracking used cross-correlation like traditional AMVs, rather than optical flow.

Assessments of EUMETSAT's IASI 3D winds product have been carried out at other NWP centres. In

¹Atmospheric Infrared Sounder

²Moderate Resolution Imaging Spectroradiometer

³Cross-Track Infrared Sounder



results shown at the 17th International Winds Workshop by Deutscher Wetterdienst, some more recent IASI 3D winds data from January 2025 were found to have O-Bs of a similar magnitude to those seen in AMVs, except for those at levels around the tropopause height and the u-component of those in the lower stratosphere, northern hemisphere. Results at the Japan Meteorological Agency, also at IWW17, showed the IASI winds were slower than the JMA NWP model, and noted problems representing the shape of wind vortices in the IASI wind data. At the US Naval Research Laboratory, two assimilation experiments were performed using the IASI 3D winds test data from February and April. While statistics of Forecast Sensitivity to Observations Impact (FSOI) indicated some benefit from the 3D IASI winds, observing system experiments showed a mixed impact from adding these wind retrievals, with degradations over the Arctic in the February experiment and over Antarctica in both experiments [1].

The aim of this report to assess the quality of the IASI 3D winds as measured by their similarity to the ECMWF IFS model background, and by their similarity to EUMETSAT's Dual-Metop AMVs, which are AMVs derived in the traditional way by use of cross-correlation between satellite images. This includes looking at bulk statistics covering the full four-month test dataset and case studies for specific observing times. Assimilation experiments were not conducted as the IASI winds were often in sharp disagreement with both the model background and the Dual-Metop AMVs, do not have a quality indicator like conventional AMVs and there would be additional work required to screen out the cloud affected IASI winds which are derived entirely from information from other sources.

2 Overview of the IASI 3D Winds Product

IASI is a hyperspectral infrared sounder on board EUMETSAT's polar orbiting Metop satellites. It has a nadir spatial resolution of 12km, and its 8,461 channels provide excellent vertical sensitivity to temperature, humidity and the concentration of trace gases including ozone. The AVHRR/3 ⁴ imager also on Metop has a finer resolution of 1.1km at nadir and observes in 6 channels. Imagery from AVHRR/3 is currently used to derive AMVs which are assimilated into the ECMWF model. For both AVHRR and IASI, as they are currently on both Metop-B and -C, the overlapping parts of the swaths from successive orbits can be used for dual-satellite retrievals.

The IASI L2 retrievals are derived in a two-step process [3]. The initial step in the IASI L2 retrieval method is called Piece-Wise Linear Regression-cube (PWLR³), is applied to both cloudy and clear-sky scenes, and works by dividing principal component IASI data into local cubes and fitting a regression model, using ECMWF NWP profiles to train the weights, giving first-guess profiles of temperature, ozone and humidity. During the first step, microwave radiance data from the MHS⁵ and AMSU-A ⁶ microwave instruments also on Metop-B/C is used to supplement IASI by providing information below the cloud tops. The cloud detection uses data from AVHRR, IASI and ECMWF short-range forecasts by comparing the observed radiances to simulated clear-sky radiances, followed usually by IASI CO2 slicing to determine the cloud height. In clear-sky areas these first-guess profiles are then overwritten with values from an optimal estimation which starts its minimisation from the PWLR³ profiles.

The IASI 3D winds are derived from IASI L2 retrievals using a variant of the optical flow technique. In general, the optical flow technique is used in machine vision applications to derive the apparent motion of objects between successive images. It assumes a constant brightness for successive images. This assumption is fine for applications involving high frame rate imagery or constant lighting conditions. For

⁴Advanced Very-High-Resolution Radiometer

⁵Microwave Humidity Sounder

⁶Advanced Microwave Sounding Unit



satellite remote sensing however, this assumption does not hold - with infrared measurements for example the temperature of the emitting objects can change between images due to heating and cooling, we cannot assume that changes over time are solely because of horizontal heat transport. Heas and Memin (2008) [5] adapt optical flow to handle brightness differences by optimising a minimisation problem that considers changes in brightness while penalising strong gradients and outliers.

EUMETSAT's 3D winds derivation is based off Heas and Memin [5] and assumes transport equations (1) in which ϕ represents humidity, temperature, and ozone information. A minimisation problem is solved for deviations from the transport equations which includes penalisation terms for outliers, horizontal vorticity and divergence gradients, and of the horizontal gradient of the vertical motion. The minimisation proceeds by alternating between the horizontal and vertical motion minimisations until convergence is deemed to have been achieved [4]. Only one wind field is derived for the three quantities temperature, humidity and ozone, which are combined together onto pressure surfaces before the wind derivation is performed. There are 25 standard pressure levels used, ranging from 13 to o1000 hPa. As with conventional AMVs tracked using cross-correlation, optical flow AMVs use the passive tracer assumption that the apparent feature motion is the same as the wind field, which will not always be true.

$$\frac{\partial \phi}{\partial x}u + \frac{\partial \phi}{\partial y}v + \frac{\partial \phi}{\partial p}\omega + \frac{\partial \phi}{\partial t} = 0 \tag{1}$$

Finally, in response to early user feedback, spatial binning is applied to the IASI winds, which reduces the variability of the wind field and aims to reduce spatially correlated error, at the expense of reducing the mean and maximum IASI wind speeds. The binning is applied using boxes of size around 100x100km, and reduces the data volume by a factor of around 25. Beyond the binning, there is no quality information or cloud mask provided with the IASI winds, nor is any quality control applied in this assessment. Consequently all figures and statistics in this report refer to all available IASI winds with no attempt made to remove poor quality IASI winds.

The test data consists of four months of IASI 3D winds data spanning January-April 2023 in a custom BUFR ⁷ format, organised into wind profiles. Although the vertical wind component was calculated during the derivation, it was not provided with the test data.

3 Overall quality assessment against ECMWF model background

To analyse the IASI 3D winds test data, it was first converted to a radiosonde BUFR format which can easily be read into the ECMWF IFS model. After being processed through IFS, each layer of an IASI winds profile ends up being treated as a separate observation.

Observation-minus-Background (O-B) statistics were calculated for the IASI 3D winds test data by running an IFS CY49R1 experiment at TCo 399 resolution (\sim 28km) covering the test data period. The IASI 3D winds were not assimilated in the experiment, meanwhile the full observing system of satellite and conventional observations was assimilated as they would be in operational use of the ECMWF model. For the assessment of the IASI winds we then use O-Bs as a proxy for quality, with the caveat that the background is not error free and its errors can increase or reduce the size of the O-Bs in some cases.

As the Dual-Metop AVHRR AMVs are derived from the AVHRR instruments on the same satellites as the IASI 3D winds, they can also be used for quality comparison against IASI 3D winds. The products are

⁷Binary Universal Form for the Representation of meteorological data



similar in that they use the overlapping swath from successive Metop-B/C orbits. The Dual-Metop AMVs are regarded as a good quality winds product [6] and are actively assimilated in the ECMWF model. However as they are cloud motion winds we cannot use them for comparison against the low stratosphere IASI winds. In the troposphere they only provide data at the trackable cloud feature locations, whereas IASI always provides a stack of complete wind layers with no gaps regardless of cloud locations.

From Figure 1 we can see that there is an overall negative speed bias in the IASI test data. Possible causes of the slow speed bias could be some combination of the smoothing terms within the derivation and the spatial binning post-processing step, though it could also be a limitation of the optical flow technique itself. Another reason why optical flow struggles to derive fast enough wind speeds could be that the passive tracer assumption does not hold as well for humidity and ozone features as it does for cloud features. The magnitude of the bias peaks at around 250-300 hPa, and has a magnitude over 5 m/s from the layers at 279 to 416 hPa, roughly corresponding to the tropopause level over polar regions. The root-mean-square vector differences (RMSVDs) also show a peak around this level at 14 m/s, whereas the uppermost Dual-Metop AMVs would have RMSVD values of around 9 m/s (Figure 2). These levels are associated with a lack of both humidity and ozone which cause the optical flow retrieval to struggle.

From the O-B peak in the O-B profile, upwards into the lower stratosphere at the layers associated with tracing ozone features, both the mean and RMSVDs are smaller. At around 100 hPa the O-B speed difference is around 2 m/s - quite small considering that there is no filtering applied to the data based on quality indicators or background check against our NWP model, as would be applied to select traditional AMVs for assimilation. This compares favourably with the mean O-B differences of the uppermost Dual-Metop AMVs, meanwhile both wind datasets have RMSVDs of around 8 m/s.

From the tropopause down to the surface the O-Bs gradually reduce from the tropopause peak. However, any information below the cloud tops will be from a combination of microwave sounder data and and the model first guess used to initialise the L2 profile minimisation.

Figure 3 splits the IASI winds O-Bs by hemisphere. Generally the O-Bs are smaller in the northern hemisphere troposphere and tropopause levels, and in the southern hemisphere low stratosphere levels. In the stratospheric layers, the difference may be coming from the higher speeds recorded in the northern hemisphere at the highest levels - around 5 to 10 m/s faster than the southern hemisphere. This may reflect the stronger polar jet over the northern hemisphere during the test data period which only covers northern hemisphere winter.

4 IASI Winds Quality at Selected Layers

4.1 Low Stratosphere

Some of the lowest O-Bs of the IASI winds data are found at the low stratosphere layers which are associated with ozone tracing.

Figure 4 shows there is general agreement between model and IASI wind speed although the IASI winds are systematically slower at all speeds, more so at high wind speeds than low wind speeds. This pattern is seen for other IASI winds from pressure layer 80 hPa down to the surface, although the magnitude of the speed difference varies. The observation versus background wind speed distribution seen in Figure 4 we can also see that the slow speeds of IASI winds compared to the model are not the result of slow outliers. This means that quality information provided with the data or a background check applied by an NWP centre would not be able to correct it, the wind speeds derived by the IASI 3D winds derivation



would need to be increased somehow.

From the maps in Figure 5 we can see that the 3D winds retrieval seems to perform well above Asia and North America, where some high wind speeds of around 30 m/s are recorded in the model and matched by the IASI 3D winds. The RMS vector difference and mean O-B difference of the IASI winds is actually higher over the lower wind speed areas such as the north pole, suggesting a problem with tracing the ozone features in these areas, rather than the tendency of optical flow to retrieve winds that are too slow.

In the example shown in Figure 6, there is good agreement between the IASI 3D winds and the ECMWF model, in terms of the general pattern of the speed and direction of the wind vectors. This includes some areas over Asia and Canada with wind speeds of 30-40 m/s. Qualitatively, it can be seen that the model wind field is smoother than the IASI wind field, for example the model shows less structure in the wind field north of Alaska than the IASI winds do.

4.2 Tropopause

At layers around the tropopause there is a lack of both humidity and ozone to provide wind information in the IASI 3D winds retrieval. Consequently it shows large differences to model wind fields at these levels. A further difficulty for the 3D winds retrieval at these layers is the presence of fast wind speeds due to the polar jet streams, which the optical flow technique struggles to capture. Figure 7 shows the effect of the IASI winds retrieval struggling to track these fast winds averaged over the 4-month test dataset, with some areas of very large (>10m/s) mean O-B speed differences in the IASI 3D winds. The Dual-Metop AVHRR winds in the same figure show much smaller O-B differences than IASI at this pressure layer, with the caveat that Dual-Metop only covers the cloudy areas while IASI winds are retrieved over all areas.

We see an example of this difficulty in Figure 8, showing IASI winds speeds far below those of the model at 280 hPa; the maximum IASI wind speed is around 45 m/s whereas the model shows widespread areas of 50 or 60 m/s wind speeds. However, in these areas the direction of the wind vectors is in good agreement with the model.

The IASI 3D winds also struggle to capture the lower wind speed areas of the wind field. For example the low and near-zero wind speeds east of the Antarctic peninsula seen in the model in Figure 8 are faster in the IASI 3D winds field. Conversely, the IASI 3D winds have an area of low or zero winds over Antarctica bounded by 60W to 0° longitude. The differences in low wind speed areas between IASI and the model could be due to a due to a lack of ozone or humidity for the optical flow to trace at this level, or that the ozone and humidity fields are too smooth for optical flow to detect the motion accurately.

4.3 Mid Troposphere

From the IASI Level 2 ATBD [3] we know that in cloudy regions much of the information from the lowest layers of the IASI 3D winds retrieval is coming from AMSU-A and MHS data with some influence from the model background used to initialise the L2 profile minimisation, rather than from IASI itself. From Figure 9 we can see that the O-B distribution of wind speeds suggests IASI winds are too slow at 525.9 hPa. As Dual-Metop AMVs are also available at this layer we can compare the distributions; Dual-Metop AMVs are centred around the y=x line and also record much higher wind speeds (25 m/s and above) than IASI which has a maximum speed of around 15 m/s. This could either be from difficulties tracing humidity features at this layer using a combination of IASI, microwave and ERA5 data, or it could be a



sampling issue due to Dual-Metop AVHRR AMVs being restricted to tracked cloud locations while IASI winds are retrieved at all locations. The stripe of very low wind speed Dual-Metop AMVs seen in Figure 9 has been linked to georegistration errors causing tracking of surface features rather than clouds [2].

In Figure 10 we can see the IASI winds are once again slower than the model in many areas, for example over central Antarctica where IASI records near-zero wind speeds and the model has wind speeds of around 10 m/s. We can also see that the structure of the wind field is different between the model and IASI winds as IASI shows a discontinuity in the Indian Ocean where the model wind field is smoother.

Figure 11 shows Dual-Metop data and corresponding model winds at the same time as Figure 10. We can see that Dual-Metop AMVs already provide good coverage at this layer, and that they are in good agreement with the speed and direction of the model winds. The fact that both the Dual-Metop AMVs and the ECMWF model show winds of around 10 m/s at this layer over central Antarctica while IASI shows 0-5 m/s suggests that the IASI winds are genuinely too slow.

5 Summary and Ideas

Background departures were generated for the IASI 3D winds test data covering January to April 2023 by processing them but not assimilating them in an experiment using ECMWF's IFS model. One main finding was that the low stratosphere pressure levels, linked to the tracing of ozone features, show reasonably low O-B values, not far from what we would consider using operationally. The main finding in the tropopause was that the 3D winds show large O-B departures at these pressure layers, indicating that the optical flow method cannot retrieve the high wind speeds of the polar jets, as well as struggling to retrieve the shape of the wind field at lower wind speeds at these layers, possibly linked to a lack of traceable features. Finally, at lower IASI winds pressure levels we saw how the Dual-Metop AMVs already do a good job of measuring the wind field as measured by O-B statistics.

Assessments of the IASI winds data undertaken at Deutscher Wetterdienst and the Japan Meteorological Agency also revealed some large background departures, albeit with a different magnitude and pattern to those shown in this report, possibly due to considering different study periods and applying quality control to the IASI winds data. Work at EUMETSAT comparing the IASI winds to Aeolus winds shows agreement with the assessment made here against ECMWF model backgrounds and Dual-Metop AMVs. We can therefore be confident the that the slow bias seen in this analysis is a genuine problem with the IASI 3D winds rather than with the NWP model backgrounds.

Some studies show that the bias is smaller when considering only the sample of IASI 3D winds after applying a relatively tight check against the model background. While such a check can be useful and justified to remove outliers, our study suggests that the bias is not caused by outliers, but rather a systematic wind-speed dependent shift in the distribution of the AMVs. A tight check against the background also introduces correlations between the errors in the observations and the background which are not accounted for in the assimilation, so we have not pursued this option in our quality analysis here.

With traditional AMVs, a model-independent quality indicator is provided based on agreement of each AMV with neighbours, and how well the subvectors between images agree with the final AMV. A quality indicator of some sort could be a useful addition to the IASI 3D winds product, though it would need to be different as there are no subvectors to consider and similarity to neighbours is already promoted during the derivation. Quality information from the IASI Level 2 retrieval could be a useful input to an IASI 3D winds quality indicator. Another useful addition would be a flag to indicate cloud affected IASI winds data points which could be done using the cloud information from the IASI Level 2 product.



From the findings of this and other assessments of the IASI 3D winds, we can see that the quality is not currently good enough to consider assimilating the data due to the large and widespread slow wind speed bias in the data and the superior quality of conventional AMVs at the pressure levels where clouds are present. The best quality IASI winds data was found in the low stratosphere, this data could be considered for assimilation in the future if quality information was provided with the IASI 3D winds, especially as they also fill in an observational gap in the stratosphere where we do not have direct satellite wind observations since the demise of the Aeolus satellite.

The question of whether assimilating wind vectors derived from infrared sounder retrievals gives a forecast improvement beyond that already provided by assimilating the IASI radiances still needs to be answered. An interesting future experiment could be to test the assimilation impact of each observation type, either for IASI radiances versus IASI 3D winds, or their InfraRed Sounder (IRS) equivalents. A further experiment to consider would be assimilating both observation types and looking for signs that assimilating the same information twice is damaging to forecast quality due to overweighting IASI observations in the analysis.

6 Acknowledgements

Francis Warrick is funded by the EUMETSAT Fellowship Programme. Thanks to Manuel Carranza, Olivier Hauteceour and Régis Borde of EUMETSAT for explaining numerous details of the IASI 3D winds derivation. Thanks also to Tomas Kral, Bruce Ingleby and Ioannis Mallas for advice and assistance on the data conversions required to put the IASI winds through IFS.

References

- [1] Brian K. Blaylock, Daniel P. Tyndall, and Patricia M. Pauley. Impact of assimilating iasi wind retrievals on navgem forecasts. Formal Report NRL/7530/FR–2024/7, U.S. Naval Research Laboratory, Marine Meteorology Division, Washington, DC, August 2024. Distribution Statement A: Approved for public release; distribution is unlimited.
- [2] James Cotton, Amy Doherty, Katie Lean, Mary Forsythe, and Alexander Cress. Nwp saf amv monitoring: the 9th analysis report (ar9). Technical Report NWPSAF-MO-TR-039, Version 1.0, NWP SAF / EUMETSAT, March 2020.
- [3] EUMETSAT. Product User Guide: IASI Level 2 TS, T, Q (Release 1). https://user.eumetsat.int/s3/eup-strapi-media/Product_User_Guide_IASI_level2_TS_T_Q_release_1_d0120f17a6.pdf, 2021.
- [4] Olivier Hautecoeur, Regis Borde, and Manuel Carranza. IASI 3D Wind Product Algorithm Theoretical Baseline Document. Technical Report EUM/RSP/TEN/23/1390583, EUMETSAT, November 2024. Version 1 Draft.
- [5] Patrick Heas and Etienne Memin. Three-dimensional motion estimation of atmospheric layers from image sequences. *IEEE Transactions on Geoscience and Remote Sensing*, 46(8):2385–2396, 2008.
- [6] K. Salonen and N. Bormann. Atmospheric Motion Vector observations in the ECMWF system: Fourth year report. *EUMETSAT/ECMWF Fellowship Programme Research Report*, No.36, 2015.



- [7] David Santek, Sharon Nebuda, and Dave Stettner. Demonstration and evaluation of 3d winds generated by tracking features in moisture and ozone fields derived from airs sounding retrievals. *Remote Sensing*, 11(22):2597, 2019.
- [8] David Santek, Elisabeth Weisz, W.Paul Menzel, and David Stettner. Determining Global 3D Winds by Tracking Features in Time Sequences of CrIS Humidity and Ozone Retrievals. *Geophysical Research Letters*, 52(11):e2025GL114680, 2025.
- [9] Laura Stewart. Derivation of AMVs from single-level retrieved MTG-IRS moisture fields. Fellows Day presentation, Met Office, March 2014. Presented on 17 March 2014; available as PDF from EUMETSAT website.



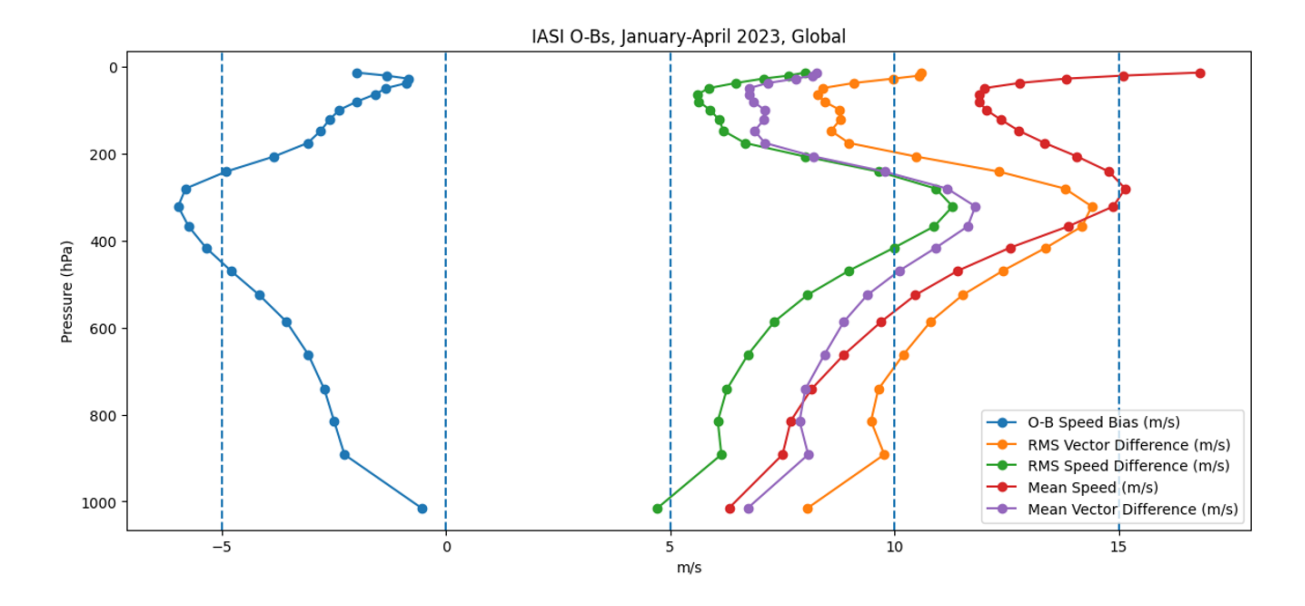


Figure 1: Global O-B statistics for the full IASI winds test dataset.

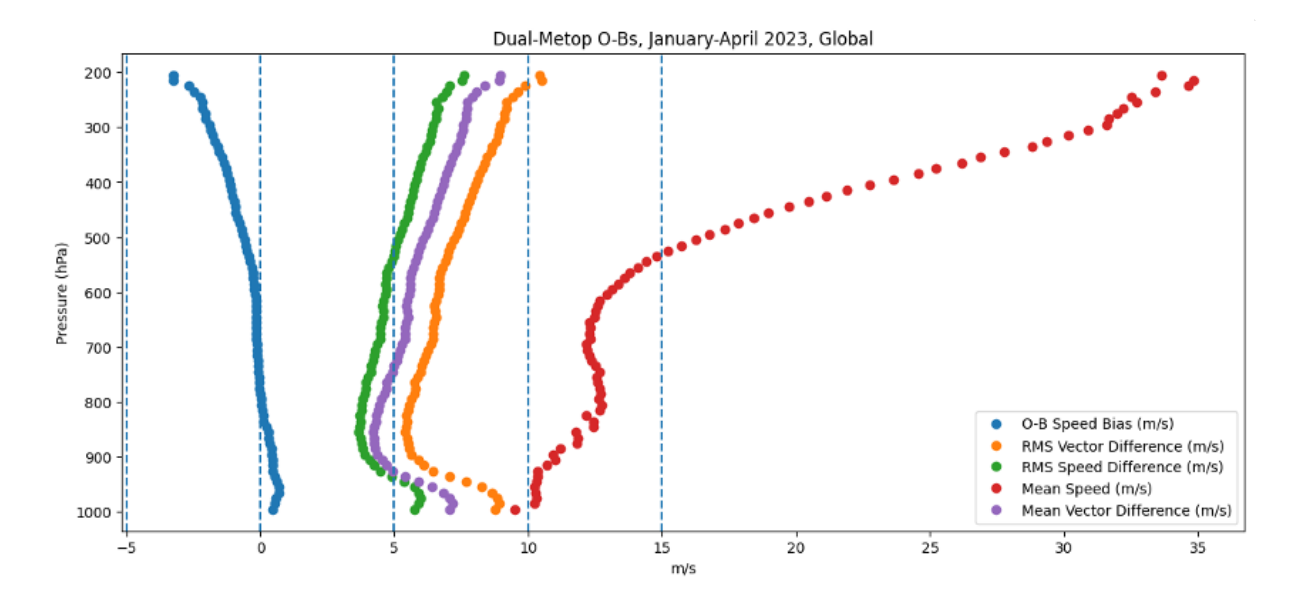


Figure 2: Global O-B statistics for the Dual-Metop AMVs, no quality control applied.



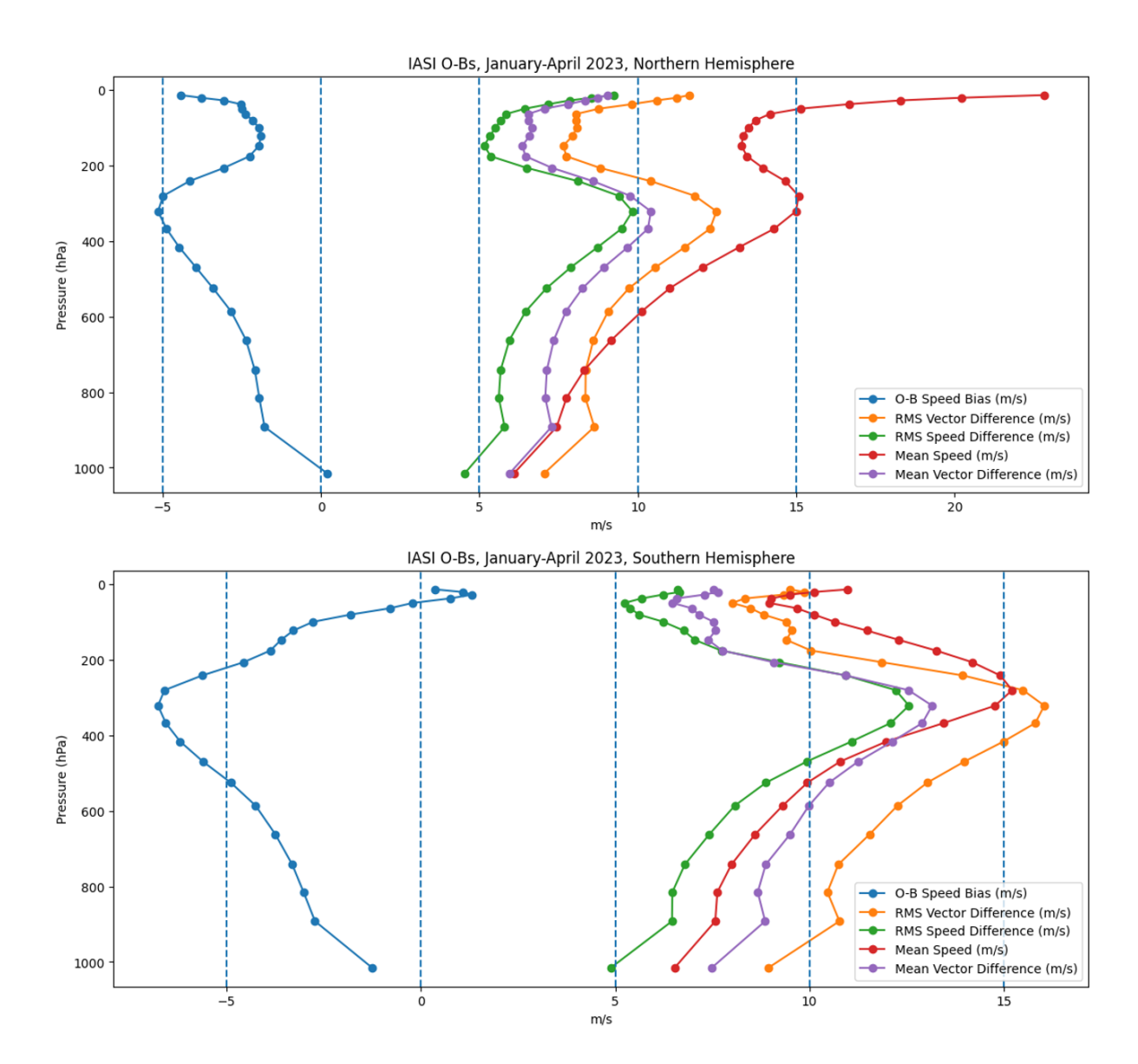


Figure 3: O-B statistics for the full test dataset, split into Northern Hemisphere (top), Southern Hemisphere (bottom).



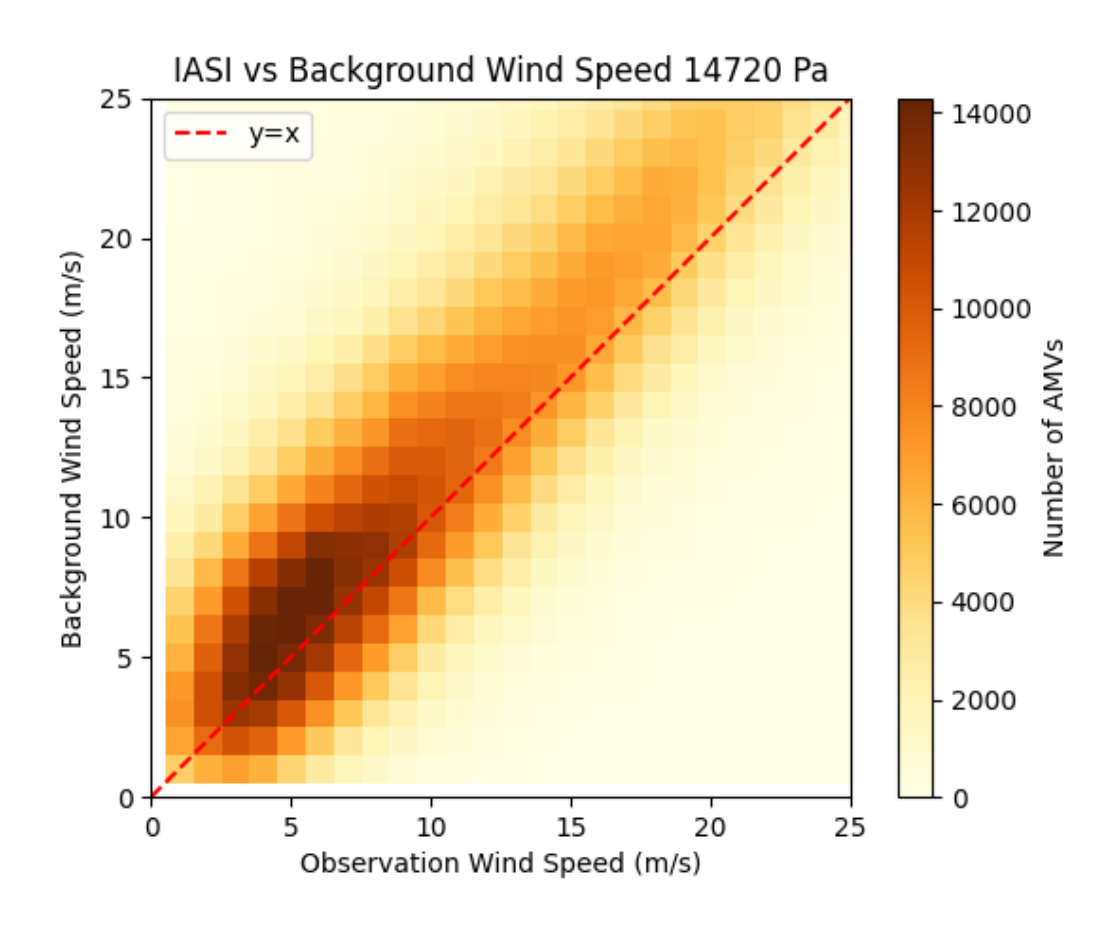


Figure 4: O-B wind speed histogram for full IASI 3D winds test dataset at 147.2 hPa.



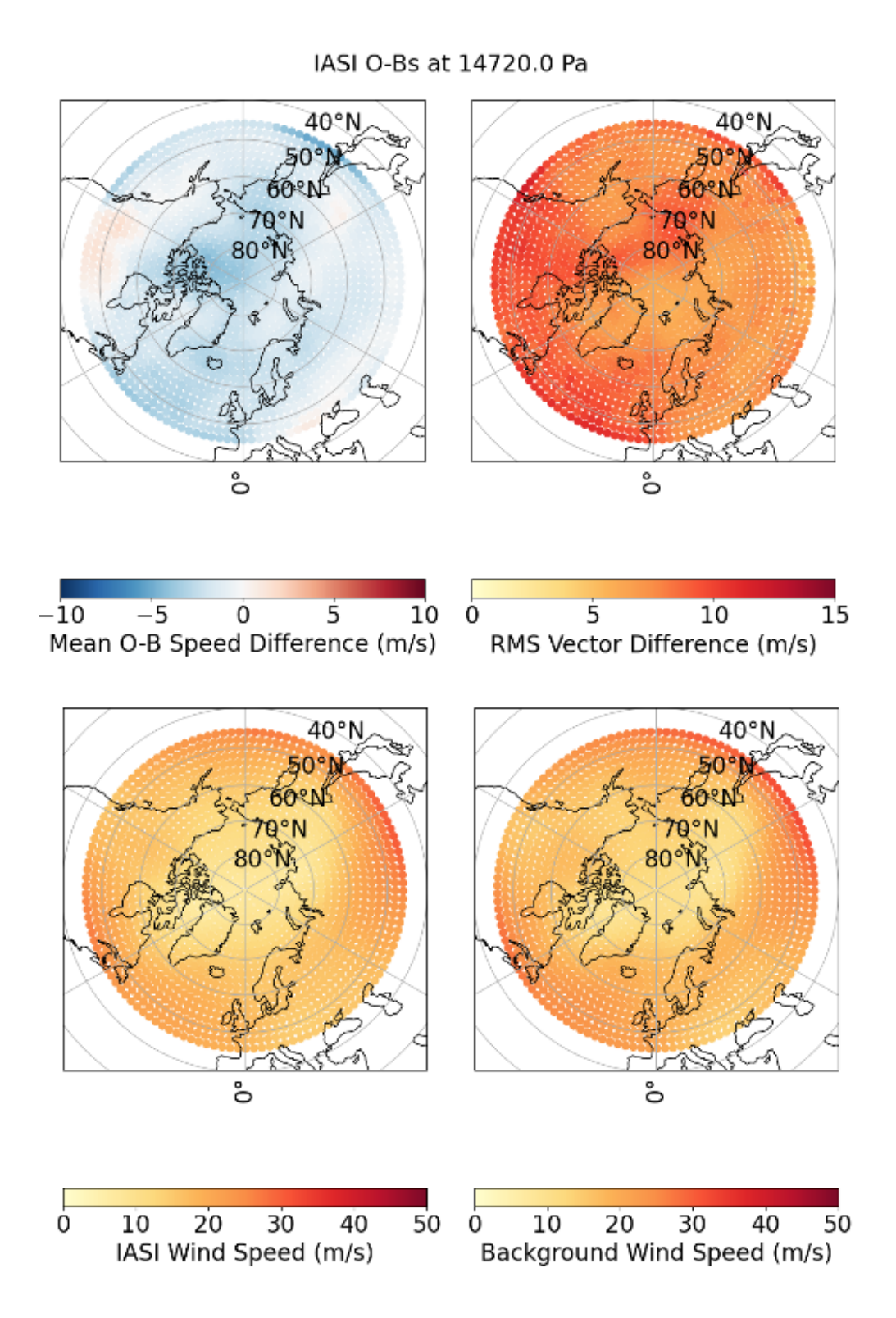


Figure 5: IASI 3D Winds O-Bs, speeds, and corresponding background wind speeds, at 147.2 hPa.



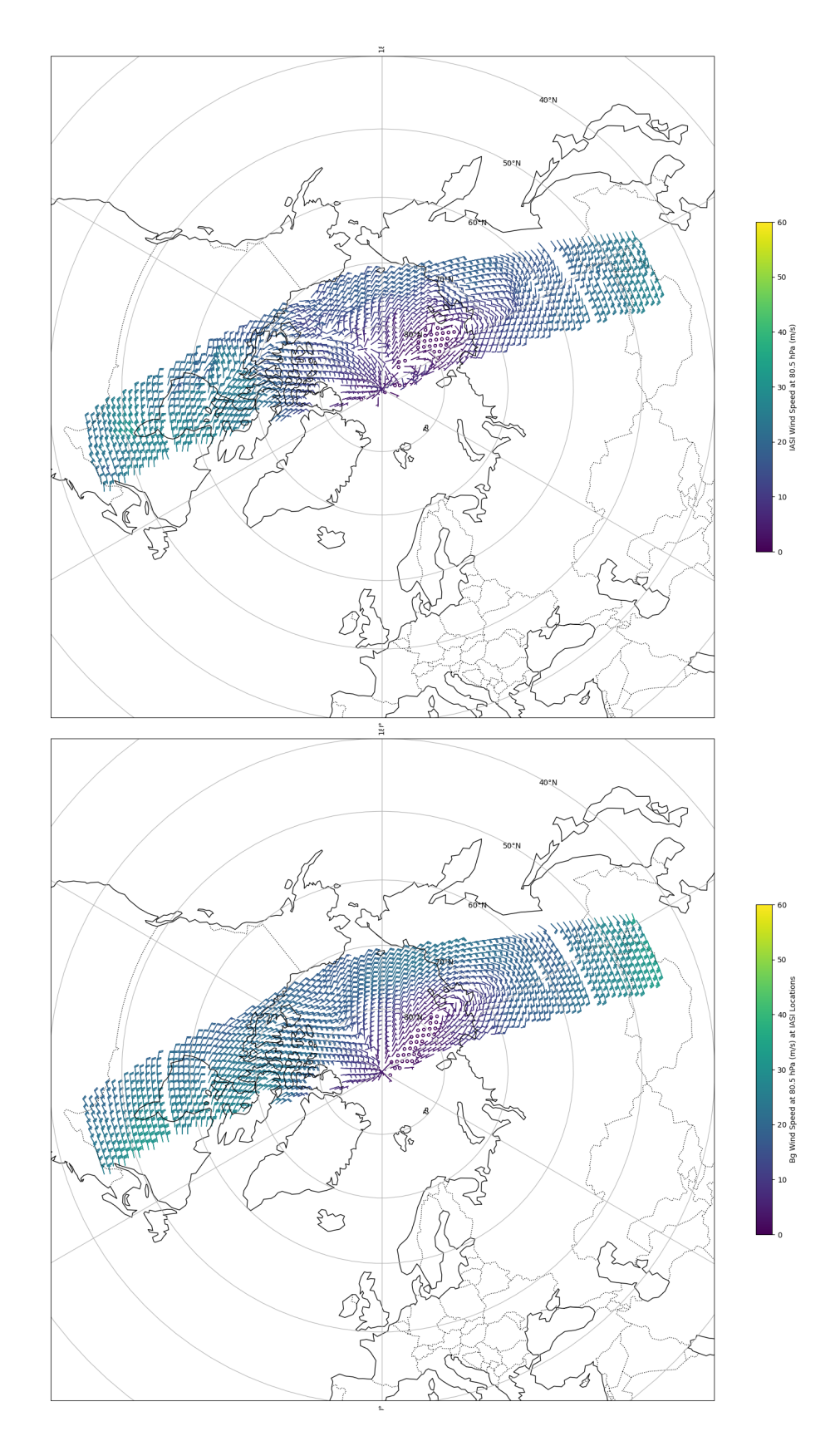
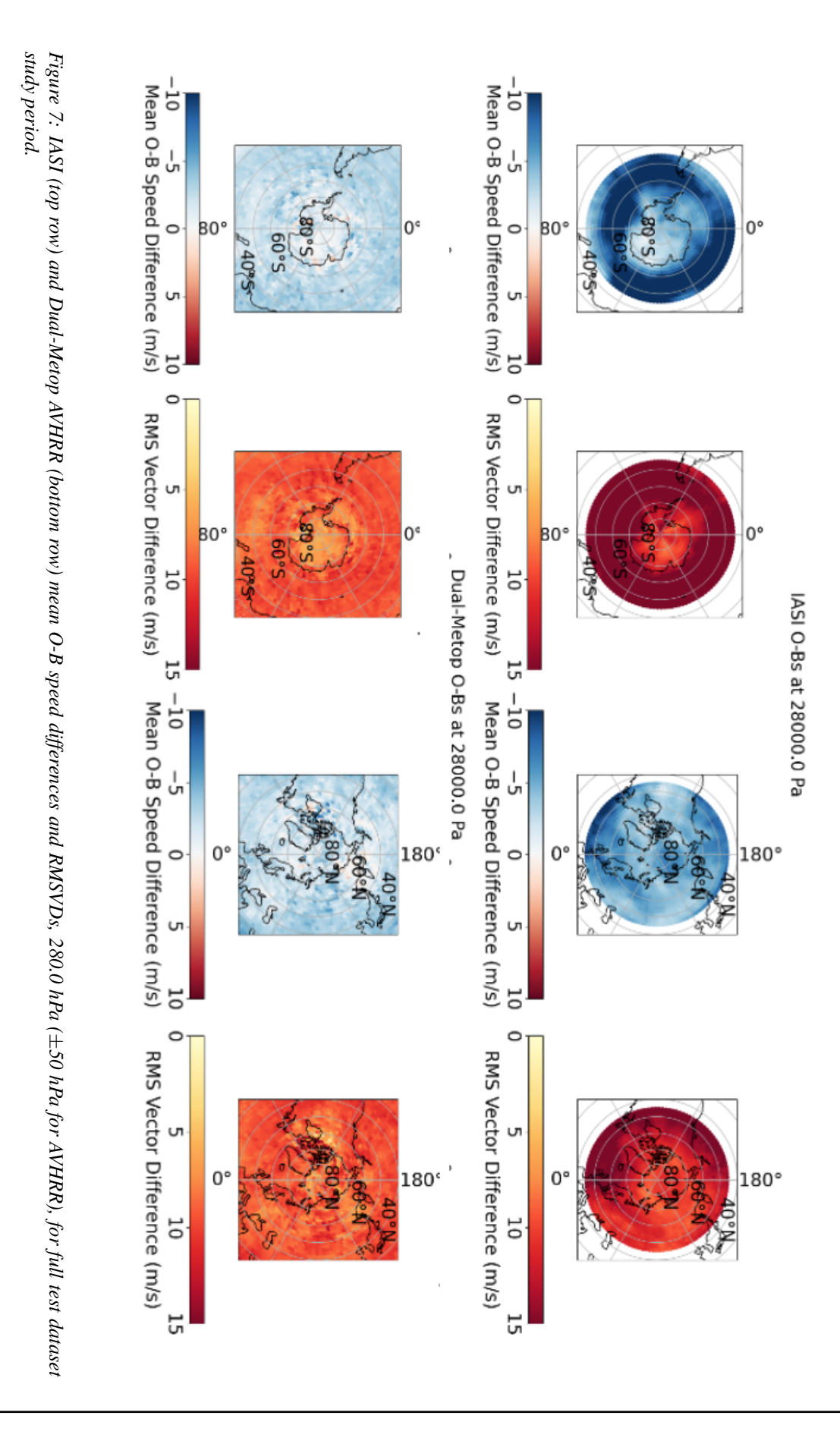


Figure 6: Wind speed barbs at 80.5 hPa for IASI 3D winds (top) and ECMWF IFS background (bottom). Data shown for 1st January 2023, 0230 to 0240 UTC.



EUMETSAT/ECMWF Fellowship Programme Research Report 66



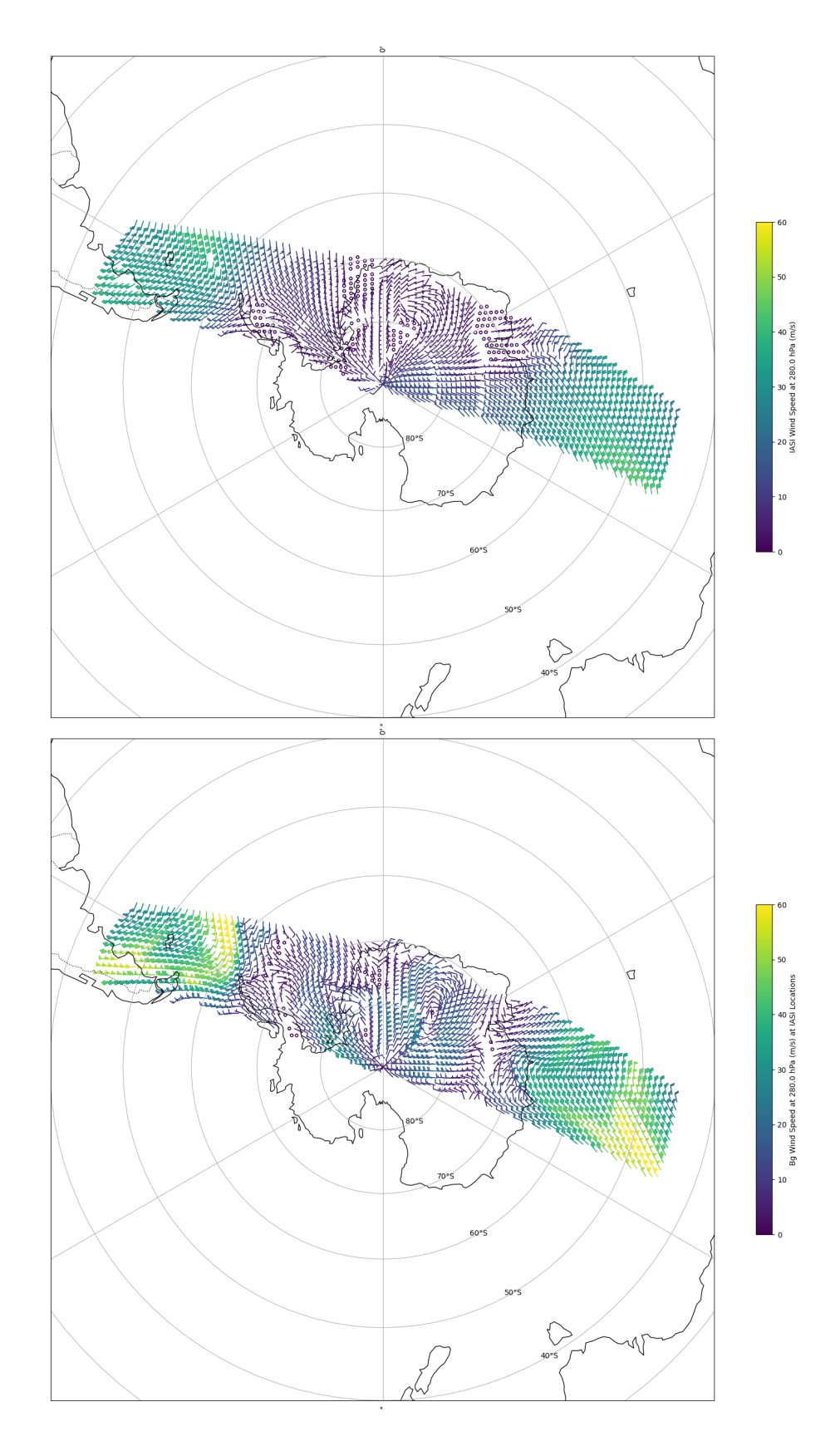
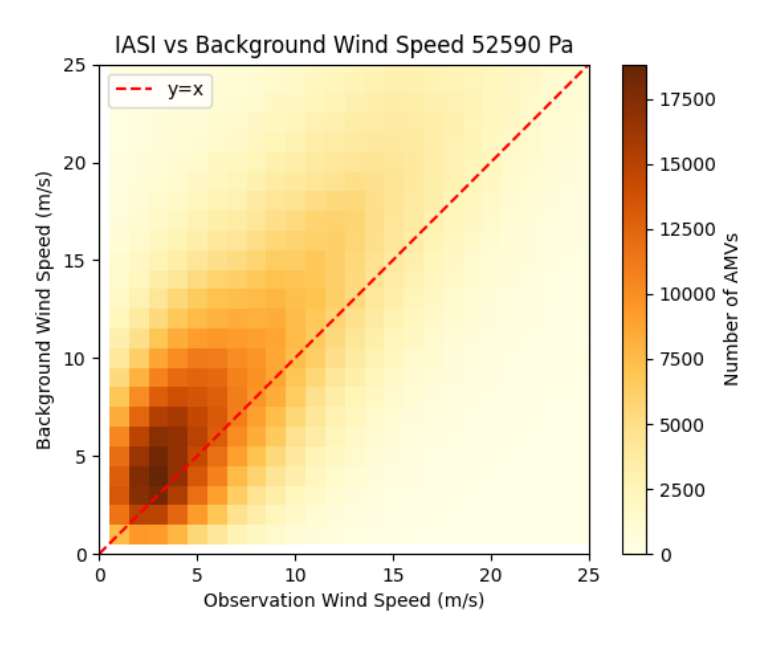


Figure 8: Wind speed barbs at 280.0 hPa for IASI 3D winds (top) and ECMWF IFS background (bottom). Data shown for 1st January 2023, 0230 to 0240 UTC.





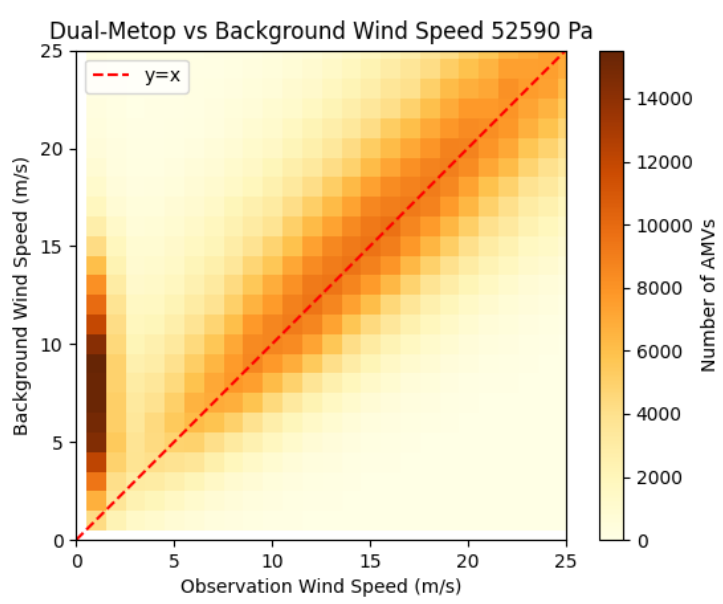


Figure 9: O-B wind speed histogram for IASI 3D winds at 525.9 hPa (top), and Dual-Metop winds at 525.9 \pm 50 hPa (bottom). Dual-Metop restricted to >45° N/S to approximate the area covered by IASI 3D winds.



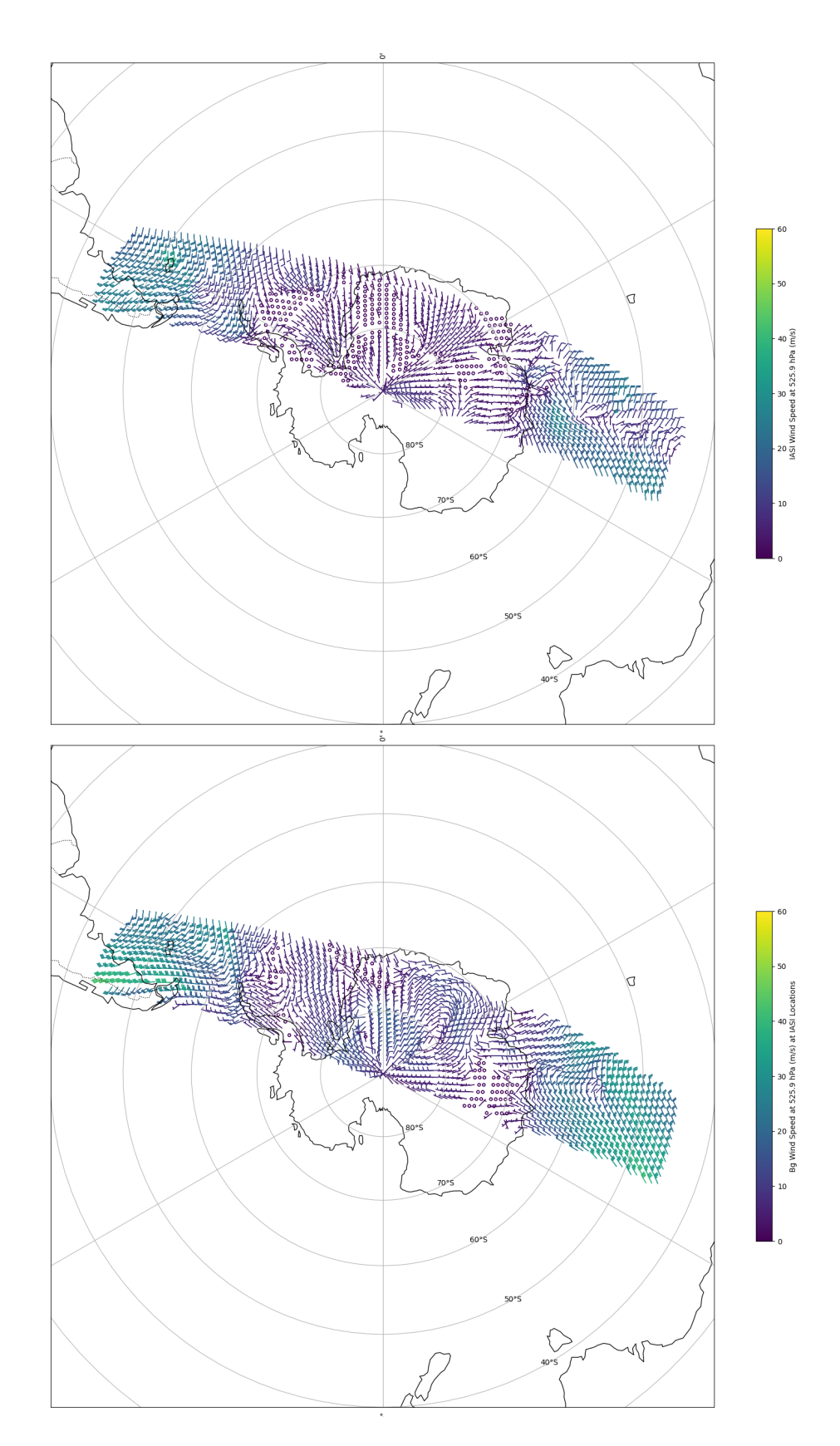


Figure 10: IASI Wind speed barbs at 525.9 hPa for IASI 3D winds (top) and ECMWF IFS background (bottom). Data shown for 1st January 2023, 0230 to 0240 UTC.



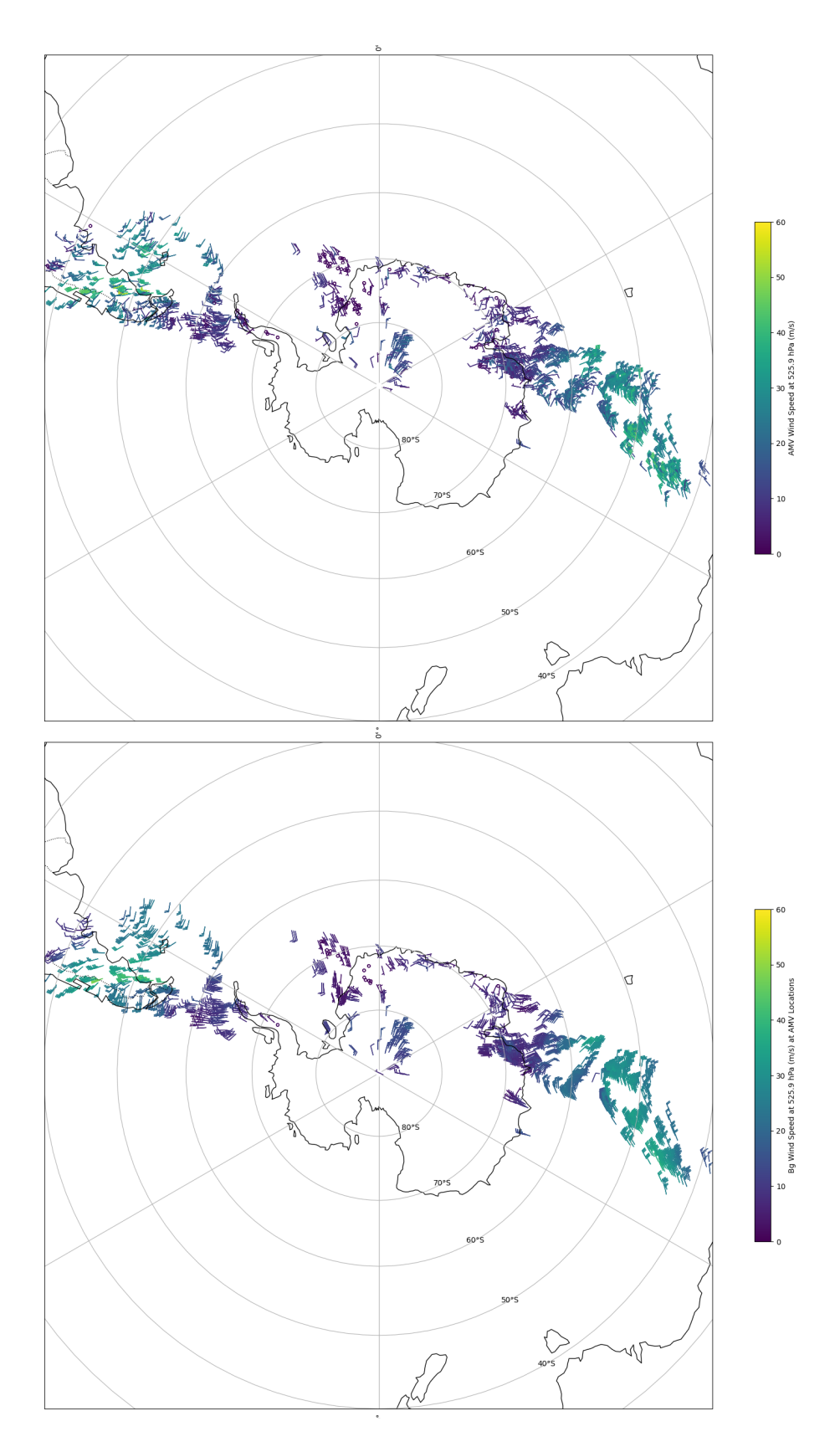


Figure 11: Dual-Metop AVHRR Wind speed barbs at 525.9 ± 50 hPa for Dual-Metop (top) and ECMWF IFS background (bottom). Data shown for 1st January 2023, 0205 to 0305 UTC.